HHS Public Access

Author manuscript

Biotechnol J. Author manuscript; available in PMC 2024 December 01.

Published in final edited form as:

Biotechnol J. 2023 December ; 18(12): e2200607. doi:10.1002/biot.202200607.

Toehold Switch Plus Signal Amplification Enables Rapid Detection

Kevin Morey[1], **Tyler Thomas-Fenderson**[2], **Al Watson**[1], **Jacob Sebesta**[1], **Christie Peebles**[1], **Claudia Gentry-Weeks**[2,*]

[1]Chemical and Biological Engineering Department, Colorado State University, Fort Collins, CO

[2]Microbiology, Immunology, and Pathology Department, Colorado State University, Fort Collins, CO

Abstract

Recent world events have led to an increased interest in developing rapid and inexpensive clinical diagnostic platforms for viral detection. Here, the development of a cell-free toehold switch-based biosensor, which does not require upstream amplification of target RNA, is described for the detection of RNA viruses. Toehold switches were designed to avoid interfering secondary structure in the viral RNA binding region, mutational hotspots, and cross-reacting sequences of other coronaviruses. Using these design criteria, toehold switches were targeted to a low mutation region of the SARS-CoV-2 genome nonstructural protein 2. The designs were tested in a cell-free system using trigger RNA based on the viral genome and a highly sensitive fluorescent reporter gene, mNeonGreen. The detection sensitivity of our best toehold design, CSU 08, was in the low picomolar range of target (trigger) RNA. To increase the sensitivity of our cell-free biosensor to a clinically relevant level, we developed a modular downstream amplification system that utilizes toehold switch activation of tobacco etch virus (TEV) protease expression. The TEV protease cleaves a quenched fluorescent reporter, both increasing the signal fold change between control and sample and increasing the sensitivity to a clinically relevant low femtomolar range for target RNA detection.

Graphical Abstract

[*]**Corresponding Author:** Claudia Gentry-Weeks, Associate Professor, Colorado State University, Department of Microbiology, Immunology, and Pathology, 1682 Campus Delivery, Claudia.Gentry-Weeks@colostate.edu.

CONFLICT OF INTEREST

The authors declare no commercial, financial, or personal conflicts of interest.

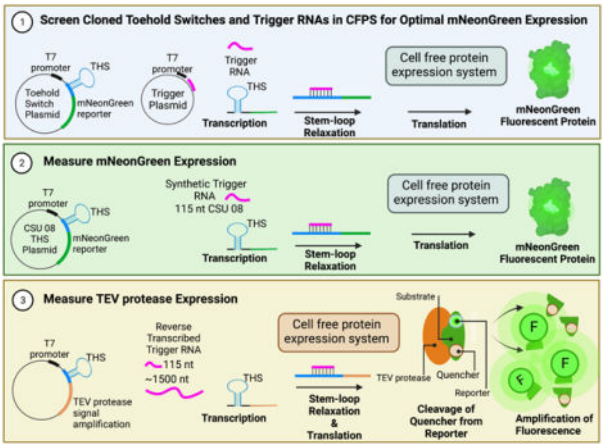

A toehold switch upstream of a fluorescent reporter gene can be used for detection of RNA viruses in a cell free expression system. When the reporter is replaced by TEV protease, the reporter signal is amplified even more since TEV protease can cleave multiple quencher-reporter combinations, resulting in significant signal amplification. In this study, the authors demonstrate that TEV protease amplification can eliminate the need for upstream signal amplification by PCR or NASBA to provide sensitive detection of SARS-CoV-2 RNA.

Keywords

Synthetic Biology; Cell Free; Diagnostics

1 INTRODUCTION

Synthetic biology offers biotechnological solutions to modern medical problems through the use of gene circuits expressed in cell-free protein synthesis systems (CFPS) for transcription and translation of a diagnostic end product.[1–3] The addition of a toehold switch to a circuit serves as an on/off switch since the resulting RNA has secondary structure, is self-binding, and can regulate the translational expression of a gene encoded on the same mRNA strand.[3] Upon interaction with a trigger molecule, the toehold switch will alter its structure to allow translation of a functional reporter protein.[2, 3]

By combining these components in a modular format, cell-free synthetic gene circuits can be easily fine-tuned to meet a specific biological or medical diagnostic need. Cell-free synthetic gene circuits have recently been developed for the detection of viral RNA particles in point-of-care devices.[2] However, large concentrations of the trigger molecule are often required for a successful diagnostic detection. We present a modular downstream amplification system for detection of viral RNA trigger sequences at extremely low sample concentrations.

As evidenced by the SARS-CoV-2 outbreak, diseases caused by RNA viruses can quickly become global pandemics.[4, 5] As a result, an increased emphasis has been placed on applying synthetic biology techniques toward rapid detection of RNA viruses. The ideal diagnostic test should be inexpensive, lack the need for lengthy antibody production or PCR amplification, and be modular in nature so it can be easily and rapidly adapted to new and

emerging threats. Current diagnostic methods rely on technical expertise, costly equipment, and often either utilize monoclonal antibodies for capture or detection, or use RT-PCR to amplify the viral RNA, which can limit the accessibility of these diagnostics to the public.[6–8] A combination of a modular synthetic gene circuit with a switch control mechanism, a downstream enzymatic signal amplification system, and CFPS offers the ability to perform rapid and sensitive detection diagnostics without the need for expensive equipment and can be adapted for distribution and storage on an inexpensive substrate such as paper.[2, 9]

Previous work established that toehold switches can form a stem-loop structure with a sequestered AUG start codon and serve as an on/off switch for expression of a downstream green fluorescent protein (GFP) reporter gene[10]. Binding of a target nucleic acid sequence (i.e. the “inducer” or “trigger”) to the toehold causes strand invasion of the stem loop structure, resulting in disruption of the stem loop structure which allows translation and synthesis of a detectable GFP. In studies by Pardee et al., a nucleic acid sequence-based amplification (NASBA) step was employed prior to the detection process to increase the amount of viral RNA trigger available for binding the toehold switch. They first amplified Zika viral RNA in the sample and incorporated a downstream β-galactosidase colorimetric signal for detection.[11] Similar strategies have been used to design toehold switches that bind SARS-CoV-2 viral RNA, resulting in translation of a detectable signal with a limit of detection (LOD) of 30 nM.[9] It is important to note that NASBA pre-amplification by Pardee et al. was required to increase the sensitivity of detection of the Zika virus synthetic trigger from 30 nM to 3 fM. In contrast, in this study, NASBA pre-amplification has been replaced by downstream amplification without the use of an additional NASBA pre-amplification step as described by previous researchers [10].

In this study, we present three different strategies for improving SARS-CoV-2 detection: 1) a downstream amplification system (Figure 1) using a tobacco etch virus protease (TEVp) detection system, 2) a quenched fluorescent reporter that is activated by TEVp cleavage , and 3) a selective design of a toehold switch to avoid both interfering secondary structure in the viral RNA trigger region and regions in the viral genome that are more likely to undergo spontaneous mutations.

For toehold switch design, rather than scan the entire SARS-CoV-2 viral genome to generate and test toehold switches, we focused on identifying regions for optimal and specific binding of viral RNA. First, a region of the viral genome for toehold design was chosen that was conserved among SARS-CoV-2 viruses but absent among human coronavirus strains that cause mild respiratory disease, such as HCoV-OC43, HCoV-229E, and HCoV-NL6 (https://www.cdc.gov/coronavirus/types.html). Second, the toehold binding region was narrowed down to avoid the pseudoknot between *orf*A and *orf*B genes, untranslated regions (UTRs), and regions with local secondary structure.[12, 13] Third, the toehold binding region was intentionally designed to avoid the structural protein genes that would be susceptible to mutation due to selective pressure from vaccination or infection.[12] The rationale for this combined, focused approach was to generate toehold switches that would be both sensitive and selective for SARS-CoV-2, would more likely remain functional even with the expected mutations associated with an RNA virus, and would bind to viral RNA sequences lacking secondary structure that might inhibit binding to the toehold switch.

Rather than use upstream amplification of the viral RNA, we opted to focus on amplification of the downstream detection signal to avoid the pitfalls associated with amplification of SARS-CoV-2 viral RNA from complicated substrates such as saliva or nasopharyngeal swabs.[14,15] For proof of concept, mNeonGreen was used as the detection signal since this fluorescent protein is three times more intense than GFP[16] and should allow more sensitive detection following binding of the toehold switch to the viral RNA. We did a preliminary test comparing the intensity of mNeonGreen to enhanced green fluorescent protein (eGFP) [17] generated in the CFPS and after 1 hour of synthesis at 37° C, the mNeonGreen sample was ca. 5 times more intense (Figure S1), an observation reported recently by Copeland et al. [18] Using this construct, toehold switches were identified that bound to SARS-CoV-2 genomic trigger RNA, allowing subsequent stem loop relaxation and translation of the reporter gene. Once toehold switches that successfully produced a positive signal using the mNeonGreen reporter were identified, a new downstream amplification system based on TEVp was engineered and tested for increased sensitivity.

2 MATERIALS AND METHODS

2.1 Design of Toehold Switch Sensors

Toehold switches were designed from the SARS-CoV-2 Wuhan strain (NCBI Reference Sequence NC_045512.2) with these parameters (Figure S2): a 3 nucleotide (nt) GGG T7 promoter enhancer sequence followed by a 12 nt toehold with an 18 nt stem sequence complementary to a 30 nt RNA trigger sequence. This was followed by an 11 nt loop containing the ribosome binding site (RBS) then 18 nt complementary to the first 18 nt stem sequence except for a start codon which occurs 6 nt after the loop. Toehold switches were designed using an iterative process either manually or with the STORM toehold switch generator software (https://storm-toehold.herokuapp.com/). An 8 amino acid linker sequence NGSAGSGH was included in all designs between the toehold switch and the reporter gene. A total of 19 toehold switches and corresponding trigger RNAs were designed for testing (Table S1 and S2, respectively).

2.2 mNeonGreen Expression Plasmid Design and Toehold Switch Sensor Synthesis

A DNA fragment containing a T7 phage promoter, an *E. coli* codon-optimized mNeonGreen gene, and a T7 terminator was synthesized by TWIST Biosciences (San Francisco, CA) in pTwist Chlor MC. An *Xba*I and a *Bam*HI site were included after the promoter and before the terminator, respectively, for directional cloning. A *Hin*dIII site 3’ to the terminator was added for cloning and/or plasmid linearizing. The construct was cloned into pUC19 to generate a high copy pUC19-mNeonGreen expression plasmid shown below (Figure 2). Toehold switches were incorporated into the mNeonGreen expression plasmid for testing with RNA triggers. Toehold switches were synthesized as part of a 117 nt forward primer using an ultramer DNA oligonucleotide (IDT, Coralville, Iowa) containing an *Xba*I site and a 19 nt region at the 3’ end complementary to the mNeonGreen gene. A reverse primer complementary to the 3’ end of the T7 terminator and incorporating a *Hin*dIII site was used with the ultramer oligonucleotide for PCR. Either Herculase II (Agilent, Santa Clara, CA) or Phusion (NEB, Ipswich, MA) high fidelity polymerases were used for the PCR reactions, according to the manufacturer’s protocols.

2.3 RNA Trigger Cloning

RNA triggers were based on the trigger design of Green et al.[10], and consisted of a 30 nt trigger sequence flanked by a stem loop structure at the 5' and 3' ends of the trigger (Figure S2).

Triggers were constructed as follows: 1) a GGG T7 enhancer, 2) a 5' stem-loop consisting of a 10 nt stem with a 6 nt loop (26 nt total), 3) a 3 nt spacer followed by the 30 nt trigger RNA sequence complementary to its respective toehold switch, 4) a 3 nt spacer, and 5) the T7 terminator which adopts a 14 nt stem and an 8 nt loop structure. The size of the RNA trigger with flanking stem-loops, GGG enhancer, and *Xba*I cloning site was 115 nt (Figure S3).

Trigger sequences were constructed in pUC19 using a process similar to that used for cloning the toehold switches (Figure 2). The trigger sequences were synthesized into an ultramer oligonucleotide (IDT, Coralville, Iowa) with an *Xba*I site and 17 nucleotides at the 3' end complementary to the 5' end of the T7 terminator. A reverse primer was constructed that was complementary to the region downstream of the T7 terminator and included the *Hin*dIII site. *Xba*I and *Hin*dIII restriction sites were incorporated into the primers for cloning the PCR product into the pUC19-T7 expression plasmid.

2.4 TEV Protease Cloning

To generate the TEVp amplification system a construct encoding the T7 promoter, the CSU 08 toehold switch, an *E.coli* codon-optimized version of the Tobacco Etch Virus protease gene and T7 terminator was synthesized in pUC57-Amp by SynBio Technologies (Monmouth Junction, NJ).

Alternative toehold switches were fused to TEVp by using an ultramer oligonucleotide with the TEVp gene incorporated. High fidelity PCR (Herculase II fusion DNA polymerase, Agilent) was then used to join and amplify the toehold switch and the TEVp. The PCR product was cloned back into the pUC57 T7 expression plasmid using *Xba*I and *Bam*HI restriction sites flanking the 5' UTR and 3' end of the TEVp gene.

2.5 Screening of Toehold Switches

The mNeonGreen expression system was used initially for comparing the functionality of the toehold switches with their respective trigger sequences. To identify the toehold switch that gave the highest readout signal, the 115 nt RNA trigger-expression plasmid was added to CFPS and co-expressed with an equal concentration of the toehold switch expression plasmid.

CFPS reactions driven by a T7 RNA polymerase expression system were assembled according to the manufacturer's instructions using the NEBExpress Cell-free *E. coli* Protein Synthesis System #E5360 (NEB, Ipswich, MA). This kit contains the T7 RNA polymerase expression system, including the necessary energy source, amino acids, translation factors, ribosomes, and a murine RNase inhibitor.

For toehold switch screening, CFPS reagents were mixed with plasmids containing the toehold switch and trigger (each at 5 nM final concentration). Reactions were conducted in 384-well plates in triplicate in 25 μl total volume per well. All mNeonGreen fluorescence detection reactions were run at 37°C to maximize the *E. coli* T7 expression system .

Two Zika toehold switches as reported by Pardee[11] et al. served as positive controls in preliminary screens.

2.6 Imaging:

See Supplementary Materials and Methods (S 2.6)

2.7 Calculation of Fold Change:

See Supplementary Materials and Methods(S 2.7)

2.8 Sensitivity Calibration and R Values

(S 2.8)

2.9 RNA synthesis of the 115 and 5,100 nucleotide SARS-CoV-2 Triggers for LOD experiments

Plasmid-free SARS-CoV2 RNA triggers were used in limit of detection (LOD) experiments. They were produced from either a *Hind*III-linearized pUC19 115 nt trigger expression plasmid or from a subgenomic SARS-CoV2 PCR amplification product flanked by a T7 promoter and terminator.

For synthesis of the 115 nt trigger RNA, *Hind*III-linearized RNA trigger expression plasmid (1 μg) was added to a 20 μl reaction volume using the HiScribe T7 High Yield RNA Synthesis Kit (NEB, Ipswich, MA #E2040S). The 115 nt trigger RNA was transcribed from the T7 promoter of the trigger-plasmid using the manufacturer's protocol, with the addition of 1 μl of murine RNase inhibitor (NEB, Ipswich, MA #M0314S). After incubation at 37° C for 2 hr, plasmid DNA was removed from the reaction using the TURBO DNase kit (Thermo Fisher Scientific, Waltham, MA # AM1907) according to the manufacturer's protocol.

To produce the 5,100 nt RNA trigger, a pUC57 plasmid containing a 6.8 kb cDNA fragment corresponding to nucleotide position 1 to 6844 of the SARS-CoV-2 genome (gift from Brian Geiss, Colorado State University) was used as the template. This region was chosen since it encompassed both regions 1 (nt 1918–1933) and 2 (nt 1865–2018) used for trigger switches and contained a larger region of the SARS-CoV-2 genome.

Ultramer oligonucleotides containing a T7 promoter in the forward primer and a T7 terminator in the reverse primer and the pUC57–6.8 kb template were used to amplify a 5,100 nt PCR product. The amplified PCR product (1 μg per 20 μl reaction volume) was mixed with reaction buffer (1X), dNTPs (final concentration 12 mM), PEG 8000 (final concentration 2%), 1 μl of Murine RNAse Inhibitor and 2 μl of T7 RNA polymerase and incubated at 37°C for 30 minutes. The template DNA was removed from the RNA reaction using the TURBO DNase kit (InVitrogen, Carlsbad, CA) according to the manufacturer's

protocol. The quality and size of the RNA was confirmed on a 2% w/v TAE agarose gel containing 1% v/v Clorox bleach stained with 0.5 mg/ml ethidium bromide according to Aranda et al.[19]

2.10 Limit of detection assays:

See Supplementary Materials and Methods (S 2.10)

3 RESULTS

3.1 Selection of SARS-CoV-2 Genome Regions for Designing Toehold Sensor Switches

A combination of strategies was used for optimal design of the toehold switches. This included identifying regions that were: 1) conserved among SARS-CoV-2 isolates, 2) unique to SARS-CoV-2 but not to common low pathogenic human coronaviruses, 3) lacking significant secondary structure that could potentially interfere with viral RNA binding to the toehold switch, and 4) not prone to mutations that could interrupt viral RNA binding.

Four conserved regions in the SARS-CoV-2 genome (nucleotide regions 1,865–2,018, 21,731–21,788, 23,536–23,598, and 27,977–28,909) were previously reported as unique to SARS-CoV-2 when compared with other coronaviruses.[12] Rangan et al. found that secondary structures were absent in the nt region 1,918 –1,933.[13] The mutation rate of this region encoding nonstructural protein 2 (nsp2) was found to be below 5% in North America, Asia, and European strains of SARS-CoV-2.[20]

Based on these considerations, this work initially focused on designing toeholds to bind the SARS-CoV-2 genome between nt positions 1,918–1,933 (TCTTGAAACTGCTCAA) designated region 1 and was expanded to include nt positions 1,865–2,018 designated region 2 (SARS-CoV-2 Wuhan strain; NCBI Reference Sequence NC_045512.2) (Figure 3). The rationale was that this region was conserved among SARS-CoV-2 isolates but absent in common coronaviruses. There was little secondary structure. Since it encoded a nonstructural protein (nsp2), it should show less variation and be under less selective pressure for mutation hotspots following vaccine usage and infections.

3.2 Toehold Sensor Switches Used for Testing

After determining the optimal target SARS-CoV-2 genome region, switches were designed as described by Green et al.[10] The location of the trigger RNA for each toehold switch design is shown on the 1,865–2,018 nt region of the SARS-CoV-2 genome (Figure 4).

3.3 In silico evaluation of toehold switches

The free energy of folding (ΔG) and conformation of the folded toehold switch sequences were measured using the RNAFold and NUPACK software packages, respectively (http://rna.tbi.univie.ac.at/cgi-bin/RNAWebSuite/RNAfold.cgi; http://nupack.org/). The predicted on/off ratios for the toehold switch designs were evaluated with STORM (Sequence-based Toehold Optimization & Redesign Model) software[21] and ranked according to the predicted on/off ratios. The on/off ratios reflect the efficiency of hybridization between the trigger and toehold switch with the ‘on’ and ‘off’ state correlating to the toehold switch plus

trigger and toehold switch minus trigger (https://storm-toehold.herokuapp.com). The toehold switch sequences, and their on/off ratios are shown in Table S1.

3.4 Screening of Toeholds and Triggers

The top 19 ranking toehold switch designs, as determined by STORM software, were tested along with their complementary triggers. Since ranking by STORM software alone may not identify the best functioning toehold switch, the toehold-trigger combinations were empirically tested using the mNeonGreen expression system in a commercially available CFPS system for production of mNeonGreen fluorescent protein. Toehold switch-plasmids were mixed with the CFPS with or without the respective RNA trigger-plasmid, and the resulting fluorescence was measured over time. A fold-change calculation comparing the ratios of the slope of the fluorescent signal change in the triggered and untriggered reactions was used to determine the significance of the on/off states of the toehold switches and to identify which toehold switches gave the highest reporter signal compared to background noise.

Toehold switch sensors (CSU 01, 04, and 08) showed a high on/off fold-change (Figure 4), that is, high relative fluorescence at the on-state but low relative fluorescence at the off-state and were selected for further experiments. The toehold switches with an on/off ratio greater than 0.3 as predicted by STORM showed the best signaling.

Toehold switch CSU 08 gave the largest, fold-changes in fluorescence, and subsequent efforts focused on this switch to save time and resources. The CSU 08 trigger RNA also corresponds to the region at SARS Cov-2 nucleotides 1,918–1,933 (region 1) which was the region that best fit all our toehold switch design criteria.

3.5 Limit of Detection with Short and Long Trigger RNA Using the mNeonGreen Reporter System.

After testing a series of trigger RNA concentrations from 5000 nM to 1 nM, we found that signaling from toehold switch CSU 08 was initiated by as little as 10 nM of trigger RNA (Figure S8). With the mNeonGreen reporter system the fold-change between background and reporter fluorescence was 1–2 fold at trigger concentrations of 100 nM to 1 fM (Figure 5). At this point it was obvious that the mNeonGreen sensor would be unreliable for the detection of RNA in clinical samples, considering that the average viral load of SARS-CoV-2 is 7.99×10^4 copies/mL (0.13 fM) in an upper respiratory tract sample and 7.52×10^5 copies/mL (1.25 fM) in a lower respiratory tract sample.[22]

This observation was confirmed while testing the ability of a larger RNA sequence to for strand displacement of toehold switch CSU 08 and production of a signal with the mNeonGreen reporter. We initially attempted to produce RNA for the first 6.8 kb of SARS-CoV-2 genome which contains trigger regions 1 and 2. We were only able to produce RNA of approximately 1.5 kb using a commercial T7 RNA synthesis kit. We discovered that there was a possible cryptic T7 terminator that stopped transcription. We moved our upper primer to start amplification downstream of the potential cryptic terminator. We also modified both the reaction conditions and reagents to obtain a long RNA transcript because commercial RNA synthesis kits are optimized for producing shorter transcripts. Thus a ca.

5,100 nt fragment (nucleotides 1,729 to 6,834 of the SARS-CoV-2 genome) flanked by a T7 promoter and terminator was amplified from a subgenomic SARS-CoV-2 cDNA. This subgenomic fragment contained the RNA trigger region for our toehold switches and was used to generate 5,100 nt trigger RNA. Fold changes for 5,100 nucleotides were comparable to the small RNA trigger (Figure 5). While the signaling fold increase for the 5,100 nt RNA trigger was slightly higher than the 115 nt RNA trigger in the fM range, none of the concentrations tested resulted in a fold increase in fluorescence of greater than 2-fold increase. These results emphasized the need to implement a different amplification strategy to improve diagnostic performance.

3.6 TEVp Assay Limit of Detection

In response to the high background noise and lack of change in mNeonGreen signal using different trigger concentrations, a new signal amplification system consisting of the TEVp gene was developed. In this system, TEVp was engineered downstream of toehold switch CSU 08 in order to proteolytically activate a quenched 5-carboxyfluorescein (5-FAM dye) reporter substrate. An *E. coli* codon optimized version of TEVp, with a 5'UTR CSU 08 toehold switch and flanked by a T7 promoter and T7 terminator was synthesized by Synbio Technologies in a pUC57 plasmid. As in the mNeonGreen reporter limit of detection experiments, the 115 or 5,100 nt triggers were tested over a 100 nM to 1 fM concentration range. Upon binding of the trigger to CSU 08 and translation of TEVp, the quenched 5-FAM fluorescent complex (i.e., QXL 520 quencher-TEVp cleavage site-5-FAM dye substrate complex) is cleaved, releasing the fluorescent 5-FAM dye. The highest fold change in fluorescence for the 115 nt RNA trigger occurred in the 100 nM reactions at 3.84 with standard deviation of 1.90, while the lowest fold change for the 115 nt RNA trigger occurred in the 100 fM reactions at 2.08 with standard deviation of 1.16 (Figure 6). Signal from the reaction could be differentiated from control reactions (experimental reactions lacking the trigger RNA) between 30–60 minute (Figure S4 and S5). In contrast to the mNeonGreen reporter system, 5-FAM was clearly induced by as little as 1 fM trigger. The fold change of 2- to 4-fold seen using the TEVp amplification system and 115 nt trigger was much better than what was seen with just the 115 nt trigger and the mNeonGreen reporter alone which showed a fold change range between 1 to 2-fold.

The highest fold change for the 5,100 nt RNA trigger occurred in the reactions with 10 nM final concentration of RNA trigger, at an average 22.79-fold change with a standard deviation of 3.92. The lowest fold change for the 5,100 nt RNA trigger occurred in the reactions with 100 nM final concentration of RNA trigger, at an average of 3.56 and a standard deviation of 0.63. The uncharacteristically low reading at the highest concentration of the RNA trigger may be due to overcrowding in the reaction and steric inhibition as these can have an inhibitory effect on translation in cell free systems.[23, 24] Alternatively, autoproteolysis of TEVp at higher concentrations, could contribute to the decrease in activity and fluorescence [25]. The 5,100 nt RNA trigger showed sensitivity down to 1 fM, indicating that we have not yet reached the lower limit of detection for the TEVp enzyme amplification toehold sensor. The 1 fM concentration of the 5,100 nt RNA-triggered reactions showed an average fold change of 15.29 and standard deviation of 1.42 when compared to the untriggered controls. These results show that the TEVp amplification system outperforms

the mNeonGreen reporter by ~15 fold at 1 fM of trigger RNA, a level that approximates the viral load in human clinical samples.

4 DISCUSSION

TEV protease is a highly sequence-specific cysteine protease from the tobacco etch virus[26] that is frequently used for the controlled cleavage of fusion proteins in vitro and in vivo. The SARS-CoV-2 detection system described here relies on strand invasion of specific target pathogen nucleic acid in toehold switches followed by in vitro translation of TEVp. The readout signal is amplified since TEVp cleaves a unique site in multiple quenched substrate molecules to provide an enhanced fluorescent signal. The advantages of this amplification system are that reactions can be run at a single temperature (4°C to 42°C) so a thermocycler is not required, nucleic acid amplification is not needed so extensive primer design and testing are not required, and added exogenous enzymes are not essential for the reaction, reducing the cost and increasing the stability of the assay. In addition, with this downstream amplification strategy, alternate enzymes can be employed for sensitive colorimetric detection and multiplexing of the diagnostic assay.

The use of toehold switches with upstream RNA amplification has been successful, reaching a limit of detection in the low, clinically relevant femtomolar level.[11, 27–29] However, point-of-care or field diagnostic assays demand an easy to use, inexpensive format that can withstand harsh environmental conditions and can be multiplexed for differential diagnoses. Although RT-qPCR, NASBA (nucleic acid sequence-based amplification) and RT-LAMP (reverse transcription loop-mediated amplification) can provide sensitive and specific detection of viruses, they each have different characteristics that may be challenging for use as low-cost, point-of-care detection assays. RT-qPCR requires the use of expensive equipment and technical expertise for precision handling of the reagents and matrix inhibitors can interfere with nucleic acid amplification. NASBA requires three enzymes - reverse transcriptase, RNAse H, and DNA polymerase - for transcribing single stranded RNA into cDNA, removal of template RNA, and production of double-stranded DNA that stimulates a signal, respectively. RT-LAMP is tolerant to matrix inhibitors; however, it requires 4–6 primers that must be carefully designed and extensively tested prior to use. In addition, RT-LAMP is not amenable to multiplexing. Matrix effects of clinical samples could also impact cell-free transcription and translation. Others have recently assessed those impacts and begun to address them in similar systems.[30,31]

In contrast, the described assay is a viable alternative, as the 5,100 nt RNA fragment was more efficient in triggering detection in the TEVp amplification system and the limit of detection was less than 15,000 copies with an approximate 10-fold change in relative fluorescence over the mNeonGreen reporter. Even with the mNeonGreen reporter, the limit of detection was lowered from a low pM range to a fM range when the 5,100 nt RNA fragment was used as the trigger. This superior performance with the larger RNA fragment was unexpected and was not due to a nonspecific effect of the 5,100 nt trigger fragment affecting toehold switch activation since inclusion of a control RNA fragment lacking the CSU 08 trigger sequence but containing flanking SARS-CoV-2 regions did not cause an increase in relative fluorescence (Figure S6; note: sensitivity calculations and R values are

shown in Figure S7). The 5,100 nt RNA trigger is extremely large compared with the size of the toehold sensor itself. This trigger region occurs near the 5' end of the 5,100 nt trigger resulting in ca. 5 kb of RNA downstream of the trigger sequence. It is possible that this extra RNA length contributes either to a crowding effect potentially enhancing trigger binding to the toehold and/or contributes to the free energy of strand invasion of the trigger RNA strand into the stem structure of the toehold switch. In a study of displacement loop formation (D-loop) in human telomere DNA, the change in the measured force-extension upon strand invasion of telomere DNA in a magnetic tweezers assay correlates with the length of the strand used for invasion.[32] Future work is needed to determine which factors such as location of the trigger sequence within the large RNA (5' end which is our case, internal or 3' end), whether secondary structure associated with the invading RNA strand is a factor (the SARS-Covid RNA has extensive secondary structure) and if there is a relationship between trigger RNA size and efficiency of toehold switch activation.

Our approach to toehold switch design, part of which was to locate potential trigger regions with little secondary structure with considerations for avoiding potential mutational hotspots and design toehold switches in those regions, differed from other efforts. SARS-CoV-2 toehold switches in other works used either an iterative design process using the whole genome, [29] protein sense sequences[9] or designed around amplicons for PCR primer pairs engineered for optimized amplification of SARS-CoV-2 [27] for upstream signal amplification. Our most successful toehold switch, design CSU 08, was based on a conserved unstructured trigger region (region 43) in the SARS-CoV-2 genome identified by Rangan et al.[13] We examined the triggers used in other studies and found a strong correlation between toehold switches with detectable signaling and their RNA triggers mapping to conserved unstructured regions identified by Rangan et al. Significantly, the best SARS-CoV-2 toehold switch sensors reported in the other studies, toehold switch S1 in Park and Lee[29] toehold switches B and F in Hunt et al.[9] and toehold switches 12 and 17 in Chakravarthy et al.[27] have RNA triggers that map to a conserved unstructured region of SARS-CoV-2. Conversely, many of the toehold switches whose triggers mapped to regions of conserved structure performed poorly (Table S1). This suggests that selecting RNA triggers from unstructured regions should be part of the design criteria when engineering toehold switch biosensors for RNA virus detection.

The specificity of the SARS-CoV-2 toehold switches described in this study remain to be tested further. However, it is worth noting that Cao and coworkers have demonstrated that toehold switch-based sensors using upstream amplification systems (LAMP/NABSA) can differentiate between subgroups A and B of respiratory syncytial virus associated with different levels of disease severity and are unable to detect closely related viruses (SARS-CoV-2, HCoV- HKU1, Rotavirus, and Norovirus-GII.4)(33). Similarly, Park and Lee found that this technology could be used for specific detection of SARS-CoV-2 and MERS-CoV virus but not closely related coronaviruses (29). Neither of these studies indicated that they had tested multiple isolates with variations in the regions binding to the toehold switches, indicating that more research needs to be performed to confirm the specificity of the test for variants. Regardless, we chose genetic regions that had been reported to have the least number of mutations and were unique to known (non-SARS-CoV-2 viruses) coronaviruses.

Supplementary Material

Refer to Web version on PubMed Central for supplementary material.

ACKNOWLEDGEMENTS

This work was supported by NIH award U01-HL152405.

DATA AVAILABILITY STATEMENT

The data that supports the findings of this study are available in the supplementary material of this article.

ABBREVIATIONS

TEVp	tobacco etch virus protease
CFPS	cell-free protein synthesis
PCR	polymerase chain reaction
RT-PCR	reverse transcriptase-polymerase chain reaction
GFP	green fluorescent protein
NASBA	nucleic acid sequence-based amplification
LOD	limit of detection
eGFP	enhanced green fluorescent protein
UTR	untranslated region
Nt	nucleotide
nsp2	nonstructural protein 2

REFERENCES

[1]. Perez JG, Stark JC, Jewett MC, Cell-Free Synthetic Biology: Engineering Beyond the Cell. Cold Spring Harbor Perspect Biol 2016, 8 (12), DOI: cshperspect.a023853v1.

[2]. Pardee K, Green AA, Ferrante T, Cameron DE, DaleyKeyser A, Yin P, Collins JJ, Paper-based synthetic gene networks. Cell 2014, 159 (4), 940, DOI: 10.1016/j.cell.2014.10.004. [PubMed: 25417167]

[3]. Hwang Y, Kim SG, Jang S, Kim J, Jung GY, Signal amplification and optimization of riboswitch-based hybrid inputs by modular and titratable toehold switches, J Biol Eng 2021, 15 (1), 11, DOI: 10.1186/s13036-021-00261-w. [PubMed: 33741029]

[4]. Baek YA, Um J, Antigua KA, Park JH, Kim Y, Oh S, Kim YI, Choi WA, Kim SG, Jeong JA, Chin BS, Nicolas HA, Ahn HJY, Shin KS, Choi YK, Park JS, Song MA, Development of a reverse transcription-loop-mediated isothermal amplification as a rapid early-detection method for novel SARS-CoV-2, Virol Sin 2020, 35, 344. DOI: 10.1080/22221751.2020.1756698. [PubMed: 32239445]

[5]. Alvarez-Munoz S, Upegui-Porras N, Gomez AP, Ramirez-Nieto G, Key Factors That Enable the Pandemic Potential of RNA Viruses and Inter-Species Transmission: A Systematic Review, Viruses 2021, 13 (4), 537, DOI: 10.3390/v13040537. [PubMed: 33804942]

[6]. Zhang D, Broyles D, Hunt EA, Dikici E, Daunert S, Deo SA, A paper-based platform for detection of viral RNA, Analyst 2017, 142, 815, DOI: 10.1039/C6AN02452A. [PubMed: 28194453]

[7]. Ma D, Shen L, Wu K, Diehnelt CW, Green AA, Low-cost detection of norovirus using paper-based cell-free systems and synbody-based viral enrichment. Synth Biol (Oxford, U.K.) 2018, 3 (1), ysy018, DOI: 10.1093/synbio/ysy018.

[8]. Pokhrel P, Hu C, Mao H, Detecting the Coronavirus (COVID-19), ACS Sensors 2020, 5 (8), 2283, DOI: 10.1021/acssensors.0c01153. [PubMed: 32627534]

[9]. Hunt JP, Zhao EL, Free TJ, Soltani M, Warr CA, Benedict AB, Takahashi MK, Griffitts JS, Pitt WG, Bundy BC, Towards detection of SARS-CoV-2 RNA in human saliva: A paper-based cell-free toehold switch biosensor with a visual bioluminescent output, New Biotechnol 2022, 66, 53, DOI: 10.1016/j.nbt.2021.09.002.

[10]. Green AA, Silver PA, Collins JJ, Yin P, Toehold switches: de-novo-designed regulators of gene expression. Cell 2014, 159 (4), 925, 10.1016/j.cell.2014.10.002. [PubMed: 25417166]

[11]. Pardee K, Green AA, Takahashi MK, Braff D, Lambert G, Lee JW, Ferrante T, Ma D, Donghia N, Fan M, Daringer NM, Bosch I, Dudley DM, O'Connor DH, Gehrke L, Collins JJ, Rapid Low-Cost Detection of Zika Virus Using Programmable Biomolecular Components, Cell 2016, 165 (5), 1255, DOI: 10.1016/j.cell.2016.04.059. [PubMed: 27160350]

[12]. Ip JD, Kok KH, Chan WM, Chu AW, Wu WL, Yip CC, To WK, Tsang OT, Leung WS, Chik TS, Chan KH, Hung IF, Yuen KY, To KK, Intra-host non-synonymous diversity at a neutralizing antibody epitope of SARS-CoV-2 spike protein N-terminal domain, Clin Microbiol Infect 2021, 27 (9), DOI: 10.1016/j.cmi.2020.10.030.

[13]. Rangan RA, Zheludev IA, Hagey RA, Pham EA, Wayment-Steele HK, Glenn JS, Das R, RNA genome conservation and secondary structure in SARS-CoV-2 and SARS-related viruses: a first look, RNA 2020, 26, 937, DOI: https://doi.org/10.1261%2Frna.076141.120. [PubMed: 32398273]

[14]. Dogan OA, Kose B, Agaoglu NB, Yildiz J, Alkurt G, Demirkol YK, Irvem A, Doganay GD, Doganay L, Does sampling saliva increase detection of SARS-CoV-2 by RT-PCR? Comparing saliva with oro-nasopharyngeal swabs, J Virol Methods 2021, 290, 114049, DOI: 10.1016/j.jviromet.2020.114049. [PubMed: 33387561]

[15]. Morais O, Alves MR, Ramos C, Ferreira F, Fernandes P, The Matrix Effect in the RT-PCR Detection of SARS-CoV-2 Using Saliva without RNA Extraction, Diagnostics 2022, 12 (7), 1547, DOI: 10.3390/diagnostics12071547. [PubMed: 35885453]

[16]. Hostettler L, Grundy L, Käser-Pébernard S, Wicky C, Schafer WR, Glauser DA, The Bright Fluorescent Protein mNeonGreen Facilitates Protein Expression Analysis In Vivo, G3 Genes|Genomes|Genetics 2017, 7 (2), 607, DOI: 10.1534/g3.116.038133. [PubMed: 28108553]

[17]. Zhang G, Gurtu V, Kain SR, An enhanced green fluorescent protein allows sensitive detection of gene transfer in mammalian cells, Biochem Biophys Res Commun 1996, 227 (3), 707, DOI: 10.1006/bbrc.1996.1573. [PubMed: 8885998]

[18]. Copeland CE, Kim J, Copeland PL, Heitmeier CJ, Kwon YC, Characterizing a New Fluorescent Protein for a Low Limit of Detection Sensing in the Cell-Free System, ACS Synth Biol 2022, 11 (8), 2800, DOI: 10.1021/acssynbio.2c00180. [PubMed: 35850511]

[19]. Aranda PS, LaJoie DM, Jorcyk CL, Bleach gel: a simple agarose gel for analyzing RNA quality, Electrophoresis 2012, 33 (2), 366, DOI: 10.1002/elps.201100335. [PubMed: 22222980]

[20]. Pachetti M, Marini B, Benedetti F, Giudici F, Mauro E, Storici P, Masciovecchio C, Angeletti S, Ciccozzi M, Gallo RC, Zella D, Ippodrino R, Emerging SARS-CoV-2 mutation hot spots include a novel RNA-dependent-RNA polymerase variant, J Transl Med 2020, 18 (1), 179, DOI: 10.1186/s12967-020-02344-6. [PubMed: 32321524]

[21]. Valeri JA, Collins KM, Ramesh P, Alcantar MA, Lepe BA, Lu TK, Camacho DA, Sequence-to-function deep learning frameworks for engineered riboregulators. Nat Commun 2020, 11, 5058, DOI: 10.1038/s41467-020-18676-2. [PubMed: 33028819]

[22]. Pan Y, Zhang D, Yang P, Poon LLM, Wang Q, Viral load of SARS-CoV-2 in clinical samples, The Lancet 2020, 20 (4), 411, DOI: 10.1016/S1473-3099(20)30113-4. [PubMed: 32105638]

[23]. Ge X, Luo D, Xu J, Cell-free protein expression under macromolecular crowding conditions, PLoS One 2011, 6 (12), e28707, DOI: 10.1371/journal.pone.0028707. [PubMed: 22174874]

[24]. Li J, Gu L, Aach J, Church GM, Improved cell-free RNA and protein synthesis system, PLoS One 2014, 9 (9), e106232, DOI: 10.1371/journal.pone.0106232. [PubMed: 25180701]

[25]. Kappust RB, Toszer J, Fox JD, Anderson DE, Cherry S, Copeland TD, Waugh DS, Tobacco etch virus protease: Mechanism of autolysis and rational design of stable mutants with wild-type catalytic proficiency Protein Engineering 2001, 14 (12), 993, DOI: 10.1093/protein/14.12.993. [PubMed: 11809930]

[26]. Polayes DA, Parks TD, Johnston SA, Dougherty WG, Application of TEV protease in protein production, Molecular Diagnosis of Infectious Diseases, Humana Press, Totowa, NJ 1998, 169, DOI: 10.1385/0-89603-485-2:169.

[27]. Chakravarthy A, Nandakumar A, George G, Ranganathan S, Umashankar S, Shettigar N, Palakodeti D, Gulyani A, Ramesh A, Engineered RNA biosensors enable ultrasensitive SARS-CoV-2 detection in a simple color and luminescence assay, Life Sci Alliance 2021, 4 (12), e202101213, DOI: 10.26508/lsa.202101213.

[28]. Köksaldı İÇ, Köse S, Ahan RE, Hacıosmanoğlu N, Şahin Kehribar E, Güngen MA, Baştuğ A, Dinç B, Bodur H, Özkul A, Şeker UÖŞ, SARS-CoV-2 Detection with De Novo-Designed Synthetic Riboregulators, Anal Chem 2021, 93 (28), 9719, DOI: 10.1021/acs.analchem.1c00886. [PubMed: 34192453]

[29]. Park S, Lee JW, Detection of Coronaviruses Using RNA Toehold Switch Sensors, Int J Mol Sci 2021, 22 (4), 1772, DOI: 10.3390/ijms22041772. [PubMed: 33578973]

[30]. Voyvodic PL, Conejero I, Mesmoudi K, Renard E, Courtet P, Cattoni DI, Bonnet J, Evaluating and mitigating clinical samples matrix effects on TX-TL cell-free performance, Sci Rep 2022, 12, 13785, DOI: 10.1038/s41598-022-17583-4. [PubMed: 35962056]

[31]. Vibhute MA, Schaap MH, Maas RJ, Nelissen FH, Spruijt E, Heus HA, Hansen MM, Huck WT, Transcription and translation in cytomimetic protocells perform most efficiently at distinct macromolecular crowding conditions, ACS Synth Biol 2020, 9 (10), 2797, DOI: 10.1021/acssynbio.0c00330. [PubMed: 32976714]

[32]. Chang TR, Long X, Shastry S, Parks JW, Stone MD, Single-molecule mechanical analysis of strand invasion in human telomere DNA. Biochemistry 2022, 61 (15), 1554, DOI: 10.1021/acs.biochem.1c00448. [PubMed: 35852986]

[33]. Cao M, Sun Q, Zhang X, Ma Y, Wang J, Detection and differentiation of respiratory syncytial virus subgroups A and B with colorimetric toehold switch sensors in a paper-based cell-free system. Biosensors and Bioelectronics 2021, 182, 113173, DOI: 10.1016/j.bios.2021.113173. [PubMed: 33773383]

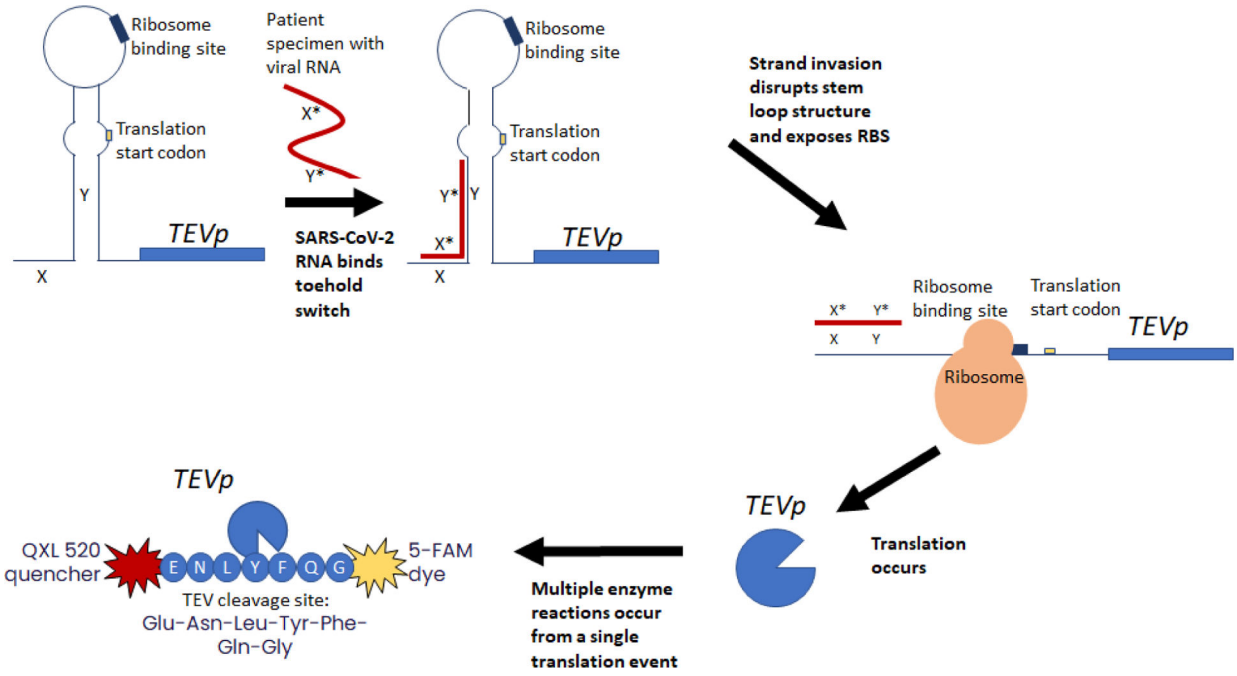

FIGURE 1.

Construction of the TEV protease amplification system located downstream of a toehold switch. The toehold switch-TEV protease transcript folds to form a stem-loop structure that blocks translation of the transcript. Following strand invasion by SARS-CoV-2 trigger RNA, the stem-loop is interrupted, resulting in translation of TEVp. A quenched fluorescent reporter is activated by TEVp cleavage and the signal fold change in fluorescence between the control and sample is measured.

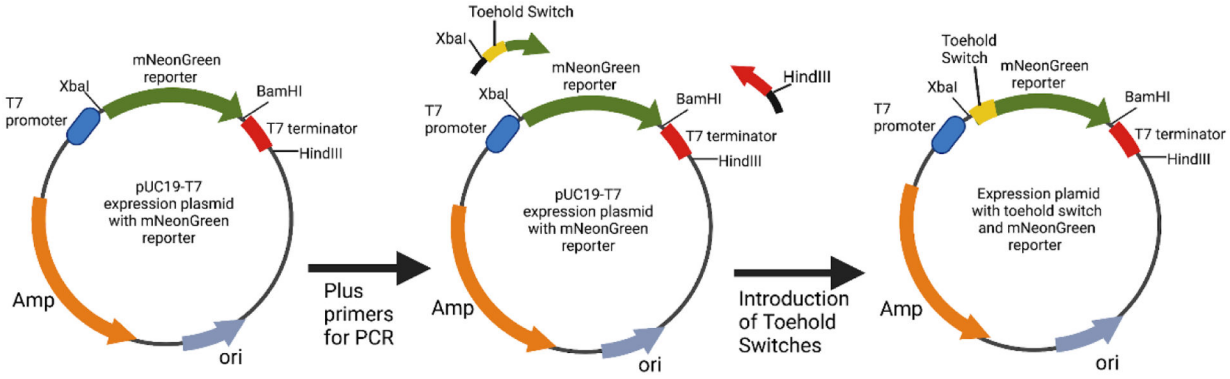

Figure 2.

Construction of the pUC19-T7 expression plasmids containing toehold switches upstream of the mNeonGreen reporter gene. A similar process was used for cloning trigger RNA sequences in the pUC19-T7 expression plasmid.

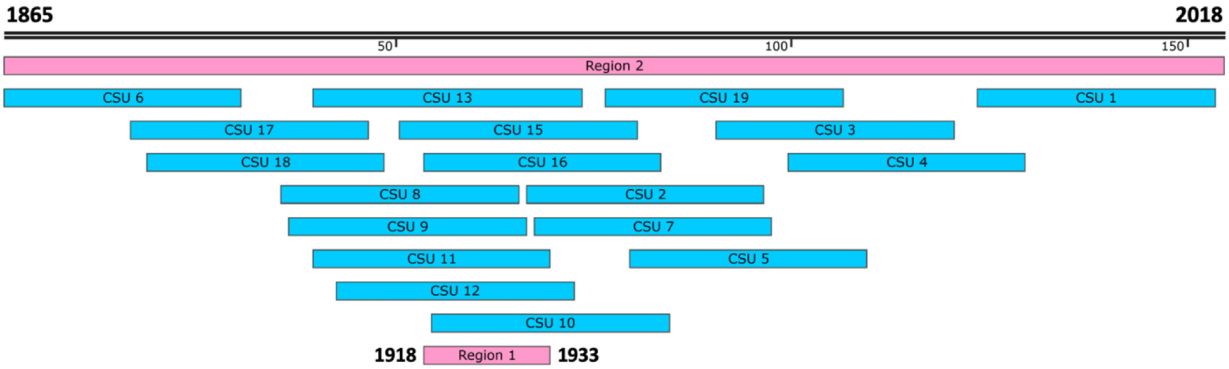

Figure 3.

Physical map of the 1,865–2018 nt region of the SARS-CoV-2 genome with the location of each trigger RNA (blue bars) for each toehold switch design. Regions 1 and 2 are indicated by the pink bars.

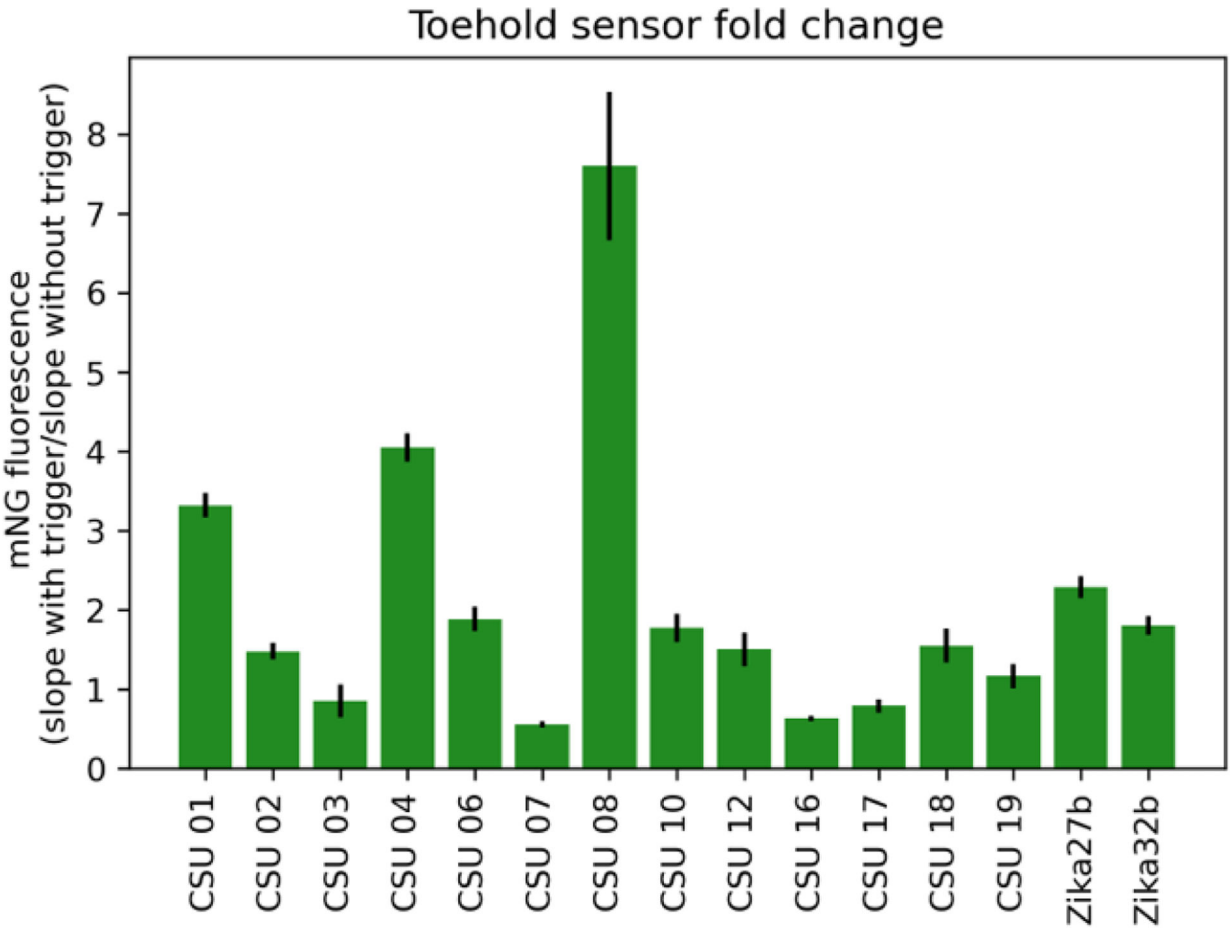

Figure 4.

Comparison of mNeonGreen fluorescence from co-expression of each toehold switch/mNeonGreen reporter with the corresponding trigger RNA in cell free extracts. Toehold switches Zika 27b and 32b were used as positive controls. Six toehold switches (not shown) gave low level fluorescence and are not included in this graph. Error bars represent +/− 1 standard deviation from the mean. The sample average and standard deviation were calculated by averaging the three technical replicate slopes for each sample, including that for the untriggered control sample (lacking the trigger-containing plasmid).

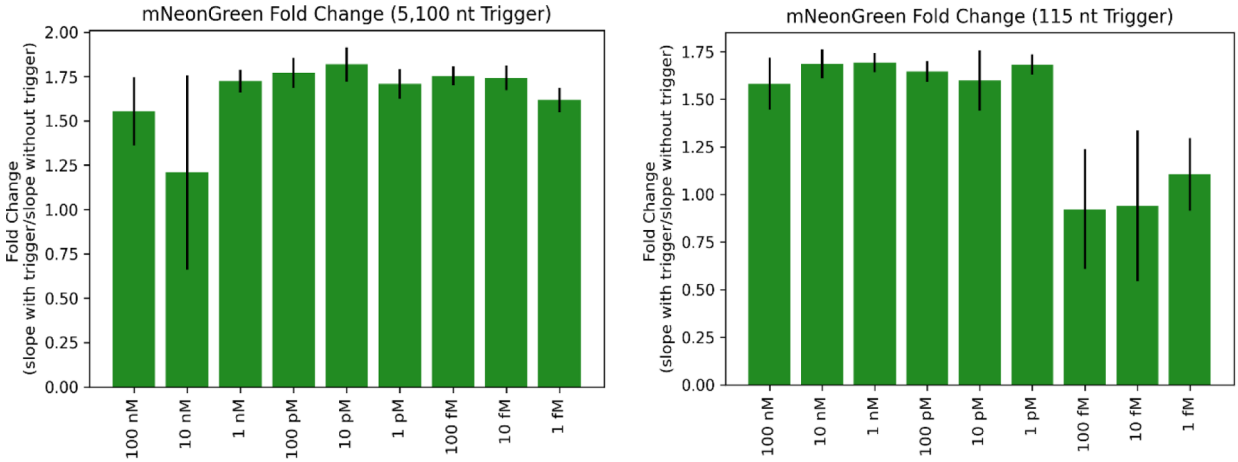

FIGURE 5.

Limit of detection dilution series using the 5,100 nt (left graph) SARS-CoV-2-derived RNA trigger and the 115 nt CSU 08 RNA trigger (right graph) with the mNeonGreen reporter. In each figure, error bars represent +/− 1 Standard Deviation from the mean. The sample average and standard deviation were calculated by averaging the three technical replicate slopes for each sample, including that for the untriggered control sample (lacking the mRNA trigger).

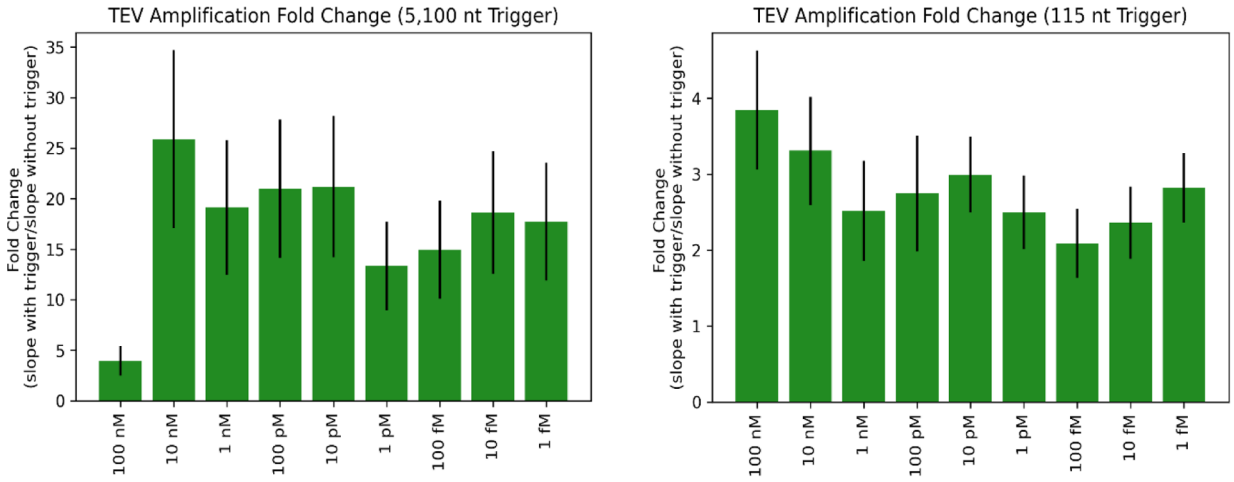

FIGURE 6.

Limit of detection dilution series using the 5,100 nt (left graph) SARS-CoV-2-derived RNA trigger and the 115 nt CSU 08 RNA trigger (right graph) with the TEV Protease reporter amplification system. In each figure, error bars represent +/− 1 standard deviation from the mean. The sample average and standard deviation were calculated by averaging the three technical replicate slopes for each sample, including that for the untriggered control sample (lacking the mRNA trigger).